



Experiments on capillary-gravity waves of solitary type on deep water

Michael Longuet-Higgins and Xin Zhang

Citation: *Physics of Fluids* **9**, 1963 (1997); doi: 10.1063/1.869315

View online: <http://dx.doi.org/10.1063/1.869315>

View Table of Contents: <http://scitation.aip.org/content/aip/journal/pof2/9/7?ver=pdfcov>

Published by the AIP Publishing

Articles you may be interested in

[Fourth-order nonlinear evolution equations for a capillary-gravity wave packet in the presence of another wave packet in deep water](#)

Phys. Fluids **19**, 097101 (2007); 10.1063/1.2772252

[Three-dimensional capillary-gravity waves generated by a moving disturbance](#)

Phys. Fluids **19**, 082102 (2007); 10.1063/1.2750293

[Three-dimensional gravity-capillary solitary waves in water of finite depth and related problems](#)

Phys. Fluids **17**, 122101 (2005); 10.1063/1.2140020

[On interfacial gravity-capillary solitary waves of the Benjamin type and their stability](#)

Phys. Fluids **15**, 1261 (2003); 10.1063/1.1564096

[The viscous damping of capillary-gravity waves in a brimful circular cylinder](#)

Phys. Fluids **14**, 1910 (2002); 10.1063/1.1476306

PHYSICS
TODAY

Welcome to a

Smarter Search

with the redesigned
Physics Today Buyer's Guide

Find the tools you're looking for today!

Experiments on capillary-gravity waves of solitary type on deep water

Michael Longuet-Higgins

Institute for Nonlinear Science, University of California San Diego, La Jolla, California 92093-0402

Xin Zhang

Scripps Institute of Oceanography, University of California San Diego, La Jolla, California 92093-0230

(Received 18 December 1995; accepted 26 February 1997)

It is shown that capillary-gravity waves of solitary type on deep water can be generated by the resonant excitation of a water surface at a speed close to the phase-speed of free waves. This speed depends upon the wave amplitude. When the source of excitation is removed, the waves are shown to propagate as free solitary waves, damped by viscosity. © 1997 American Institute of Physics.
[S1070-6631(97)00107-4]

I. INTRODUCTION

The existence of a progressive, irrotational capillary-gravity (CG) of *finite* amplitude, and of solitary type, on deep water was predicted on physical grounds by Longuet-Higgins¹ who derived a rough approximation to its speed and profile. This was a solitary wave of limiting amplitude, enclosing an “air bubble” in its trough. By accurate numerical computation² it was later shown that this was one of a theoretical family of solitary waves whose phase-speed c depended on their amplitude, or on the maximum angle of inclination (α_{\max}) of the surface; see Fig. 1(a). Moreover as α_{\max} decreased, c increased and was always *less* than the minimum phase-speed $c_{\min} = (4gT/\rho)^{1/4}$ for waves of infinitesimal slope. Here g denotes gravity, ρ the density and T the surface tension of the fluid. The dependence of α_{\max} on c for wave symmetric about a central trough is shown in Fig. 2.

Vanden-Broeck and Dias,³ using a different numerical method, verified these results and extended them to waves of smaller amplitude; see Figs. 1(b) and 1(c). The approximate dispersion relation

$$c = c_{\min}(1 - \frac{11}{64}\alpha_{\max}^2) \quad (1.1)$$

was derived by Longuet-Higgins⁴ for waves of sufficiently small slope. It was shown also that for small slopes the waves can be considered as wave packets in which the group-velocity equals the phase-velocity.

Experimentally, CG waves of solitary type have been detected in a wind-ruffled laboratory channel by Zhang and Cox.^{5,6} The phase-speed of these waves was not measured, however. There is reason to think that they are a common component of the small-scale structure of the sea surface at low and moderate wind-speeds.

In the present paper we shall describe some experiments to test whether waves of solitary type can be generated under controlled conditions in the laboratory.

II. APPARATUS

In studying the propagation of a free, or nearly free, solitary wave of very short wavelength it is desirable to find a means of excitation that is not unduly intrusive. With periodic capillary waves one can use the dispersive properties of the wave to produce a semi-infinite wave train which may

be studied at a distance from the wavemaker, but with a solitary wave the method of generation must be local. As the initial source of wave energy we therefore chose a localized jet of air impinging on a steady current in a flume. After generating the wave the jet was then switched off, leaving the wave to propagate freely under the action of viscosity.

Figure 3 is a sketch of the flume used in the experiments. Water circulated in a horizontal channel of maximum depth 36 cm, width 10.3 cm and overall length 2.6 m. The working length was 2 m. The maximum velocity in the channel was 1 m/s, but operating speeds in these experiments were always less than 25 cm/s. The uniformity of the horizontal velocity was tested by inserting particles of dye (rhodamine) simultaneously at different positions across the tank, and observing the resulting deformation of the dye traces. This also provided a measure of the turbulent fluctuations in the flow. The measurements indicated that except within a layer close to the walls and bottom (of order 0.2 cm) the current speed was uniform to within about 1 percent.

Above the channel was placed a rectangular air chamber of external dimensions 8 cm × 10 cm × 15 cm, made of plexiglass 2 mm thick; see Fig. 4. Air was drawn into the chamber by a small electrically driven pump mounted at the top of the chamber. The air exited at the bottom through a narrow slit whose width was adjustable, normally about 1 mm. A honeycomb slab 3 cm thick was placed in the chamber to suppress turbulence. The whole chamber was mounted on an electrically driven trolley capable of moving at a uniform horizontal speed. In the experiments to be described the trolley remained at rest.

The air pressure in the chamber was monitored by means of a manometer attached at the back and not shown in Figure 4. Normally the additional air pressure was less than 3 mm of water.

To visualise the wave profile, the water surface was illuminated from below, through the transparent bottom of the channel, by means of a 5 cm slide projector; see Fig. 3. The light was made to pass through a narrow slit in an otherwise darkened slide, and was focussed on the water surface, producing a sheet of light in a vertical plane parallel to the current. A visible profile of the water surface was obtained

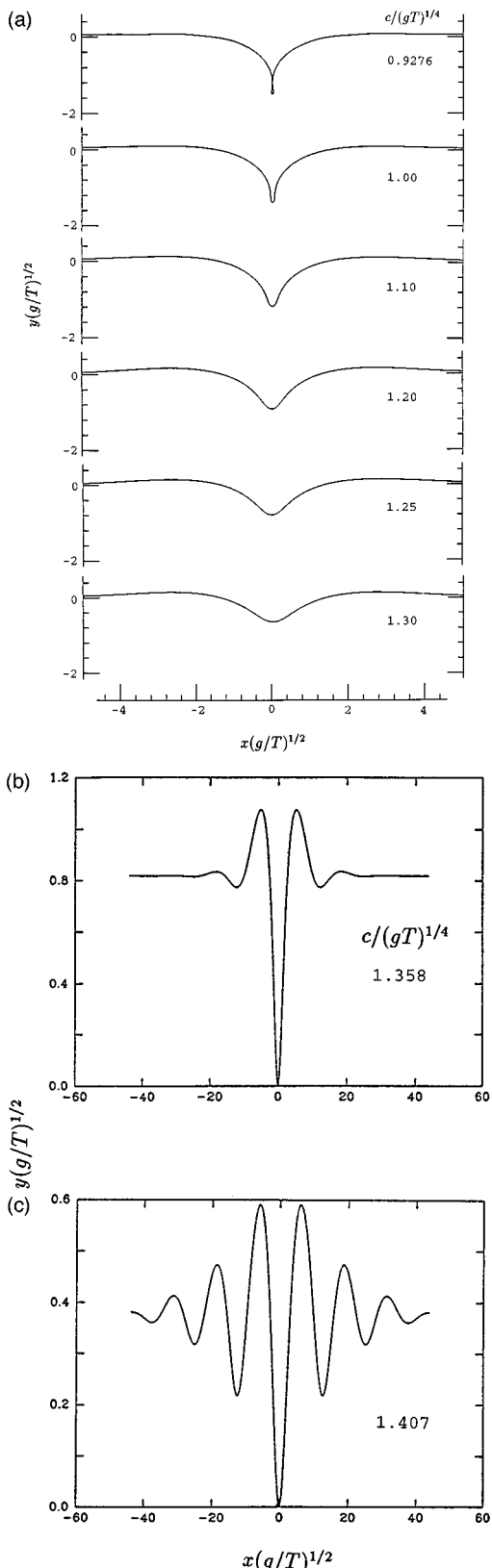


FIG. 1. Computed profiles of solitary capillary-gravity waves on deep water (a) from Longuet-Higgins (Ref. 2) and (b) and (c) from Vanden-Broeck and Dias (Ref. 3).

by scattering on the surface a small quantity of chalk powder, at a point well upstream. On passing over the projector, a section of the surface about 15 cm wide became clearly visible.

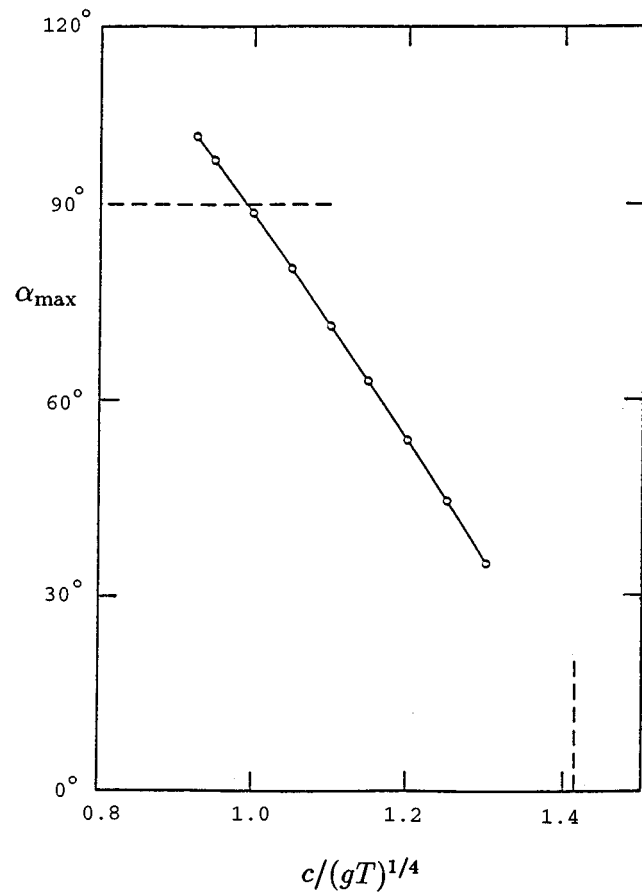


FIG. 2. Dependence of the maximum surface slope upon the phase-speed c , for trough-symmetric solitary waves.

III. EXPERIMENTAL PROCEDURE

The pressure chamber was first situated at a point near the centre of the working section of the fluid, and the water level was then adjusted so that the least distance between the air chamber and the water surface was about 5 mm. This

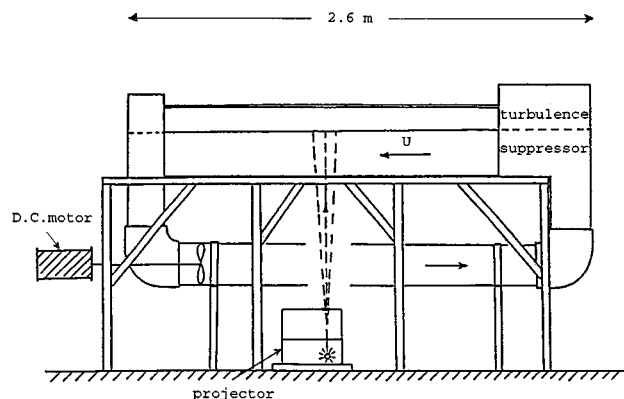


FIG. 3. Sketch of circulating water channel, showing impeller, turbulence suppressor and method of illumination.

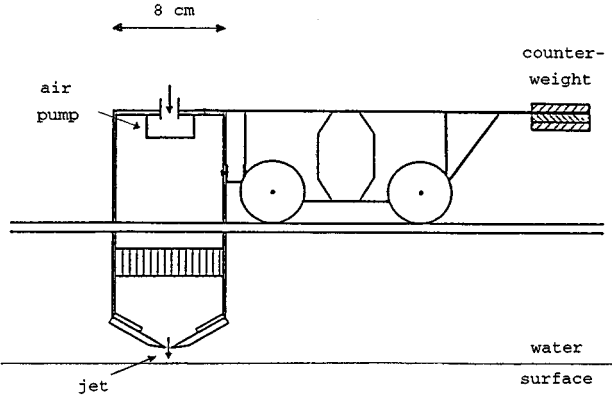


FIG. 4. Sketch of pressure chamber to produce a thin jet of air impinging on the water surface.

distance was determined by the consideration that the half-width of the pressure distribution of the air on the water surface should be comparable with the horizontal scale of a solitary wave, that is of order $(T/g)^{1/2}$, or 2.7 mm. The air flow near the jet was assumed to be approximately as in Fig. 5(a). This shows the streamlines from an aperture of width $2d$ ($d=0.1h$) at a height h above a plane surface, assuming the flow to be irrotational. The velocity (u, v) is given by the expression

$$(u - iv) = i \sum_{n=0}^N \left\{ [d^2 - (z - 2n+1ih)^2]^{-1/2} \right. \\ \left. - [d^2 - (z + 2n+1ih)^2]^{-1/2} \right\}. \quad (3.1)$$

The first term ($n=0$) in the summation represents the flow through the gap $(i-d, i+d)$ in the absence of any other boundaries, together with its reflection in the line $y=0$. The remaining terms in the series are added to ensure zero additional flow across the barriers $(i-\infty, i-d)$ and $(i+d, i+\infty)$.

Figure 5(b) shows the velocity distribution along the plane $y=0$, and Fig. 5(c) shows the distribution of the pressure. The half-width of the pressure distribution is $0.48h$, and this is almost independent of the width of the gap, when d/h is small.

Great care was taken to ensure that the water surface was clean during the experiment. Before each run the flume was emptied and refilled with fresh water, and the surface meniscus, which usually began to form at the downstream end of the channel, was removed and controlled by a vacuum-cleaner intake held about one centimeter above the surface at the downstream end.

The water speed in the channel was determined by timing the passage of a vertical dye-streak (c.f. Section II) between two points spaced 1 m apart on either side of the center point of the channel. The speed U was calibrated against the voltage supplied to the electric motor driving the impeller. Similarly the pressure in the air chamber was calibrated against the voltage supplied to the rotary air pump.

During a run, the surface displacement was first observed with the water stationary and it was checked that the vertical displacement of the water surface was negligible

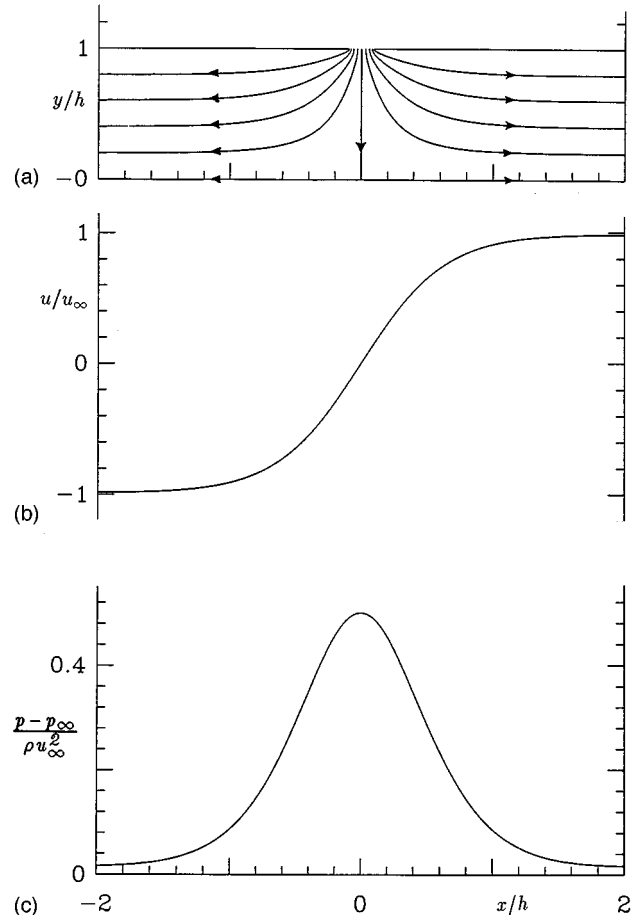


FIG. 5. Simple model of the flow field in the air as given by Eq. (3.1). (a) Streamlines, (b) horizontal velocity at $y=0$, and (c) pressure distribution on $y=0$.

(less than 0.2 mm). Small surface currents could however be observed flowing outward from the region of the jet, due no doubt to the horizontal friction of the air. Their magnitude was of order 1 cm/s. This was very probably reduced when the water was in mean horizontal motion. For, there would be less time for the transfer of horizontal momentum from the air to the water.

IV. RESULTS

On setting the water in motion with a horizontal surface velocity U somewhat below the minimum speed of linear CG waves (23 cm/s), the observed effect on the surface profile was quite dramatic. As shown in Fig. 6, a V-shaped depression appeared beneath the jet, similar in form to the profile of a solitary CG wave having the same phase-speed U . Figure 7 shows a superposition of the profile in Fig. 6 on one of the theoretical profiles in Fig. 1. The agreement is close.

The profile was not completely steady, however. Especially at lower current speeds U , there appeared from visual observation to be persistent lateral instabilities taking the form of transverse progressive or standing capillary waves of short wavelength, propagated across the channel. This led to a considerable scatter in the observed profiles. Accordingly

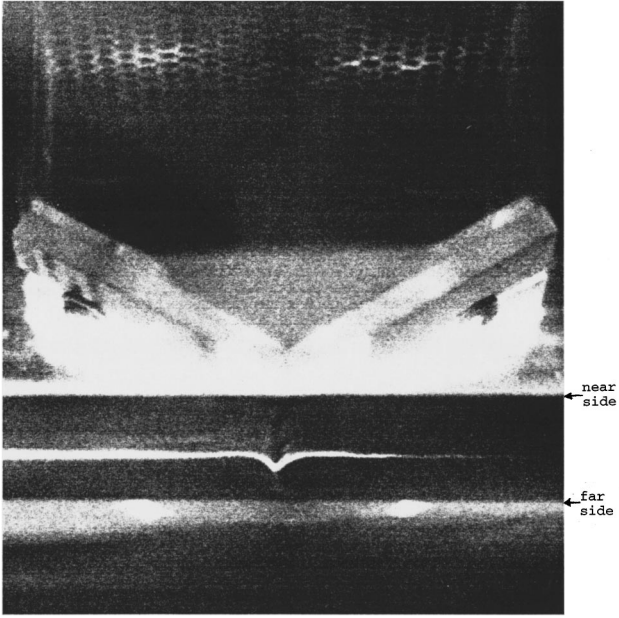


FIG. 6. View of water surface taken from slightly below the mean level, looking upward at an angle of 25° to the horizontal. The water moves to the left at a speed of 17 cm/s.

at each value of the current speed U several high-speed photographs of the surface profile were taken. These were subsequently digitized, a slight numerical correction being made for the non-horizontal angle of viewing. To find the surface slopes, some smoothing was applied before differentiation. The resulting values of α_{\max} and α_{\min} have been plotted in Fig. 8 against the current speed U . The full curve represents the theoretical calculations by Longuet-Higgins² and the broken curve the asymptote (1.1) for low values of α_{\max} . It will be seen that for current speeds U greater than about 20 cm/s, when the theoretical values of α_{\max} do not exceed 40° , the observed values follow the theoretical curve reasonably well. However for current speeds U less than 20 cm/s the maximum slopes are not much different from those at 20 cm/s and they fall significantly short of the theoretical values. We attribute this to the fact that at larger values of α_{\max} the surface profile is less well matched to the forcing pressure, indicated in Fig. 5(c). Indeed, over part of the profile the applied pressure may tend to reduce the wave amplitude.

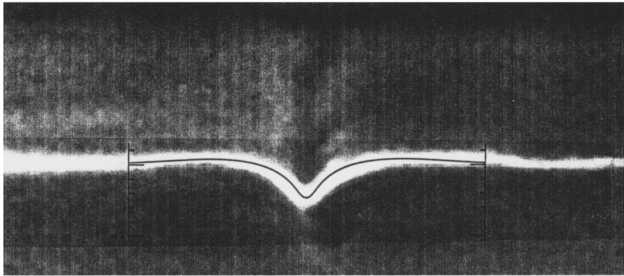


FIG. 7. Comparison of the observed profile in Fig. 6 with the corresponding theoretical profile in Fig. 1.

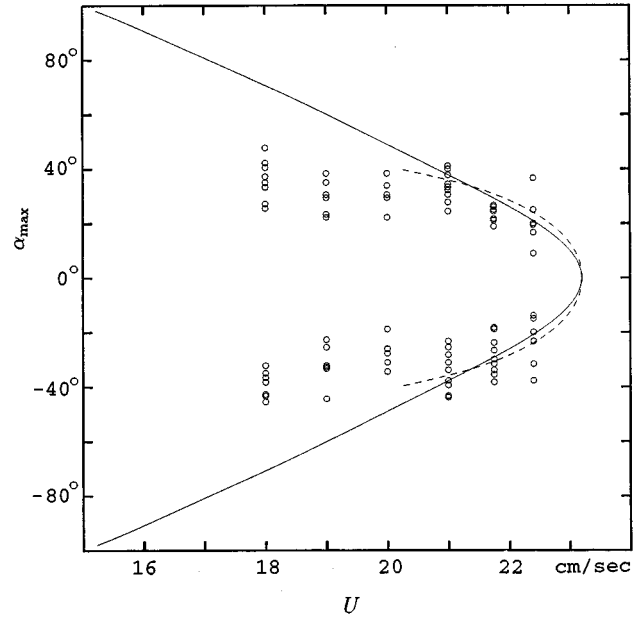


FIG. 8. Plot of α_{\max} and α_{\min} against the current speed U . The full curve corresponds to the theoretical calculations in Fig. 1, with $c=U$. Dashed curve is the asymptote (1.1).

V. FREE DAMPED WAVES

To determine the behaviour of the solitary waves when the exciting force is removed a further experiment was performed in which the jet of air was sharply cut off and the subsequent surface profile was observed over a time interval of up to 2 s. The waves being subject to viscous dissipation, we expect their amplitude to diminish gradually in time. From Fig. 2, we also expect the phase-speed to *increase*. Since in the steady state of Fig. 6 the wave is travelling to the right relative to the steady current, when the amplitude is allowed to diminish we expect the wave will move upstream, that is to the right, at an increasingly greater speed.

Figures 9(a) to 9(l) show exposures of the surface profile, made at intervals of 0.1 s, from the same position relative to the flume. The vertical arrow above each frame indicates the horizontal position of the main wave trough. The wave amplitude was measured in two ways. In the first four frames, 9(a) to 9(d), the profile was overlaid by one of a set of theoretical profiles, similar to those in Fig. 1(a) but more closely separated, thus obtaining the wave height and the associated maximum slope α_{\max} . In the remaining frames, 9(e) to 9(l), the maximum and minimum slopes were measured directly. Where the two differed in magnitude, due to background noise or other cause, the average of the magnitudes was taken. The resulting slopes are plotted against time in Fig. 10.

In Fig. 10 is also shown a theoretical curve derived from the calculated dissipation of energy D and the known energy E in a steady, solitary capillary-gravity wave,⁷ from the equation

$$\frac{dE}{dt} = -D \quad (5.1)$$

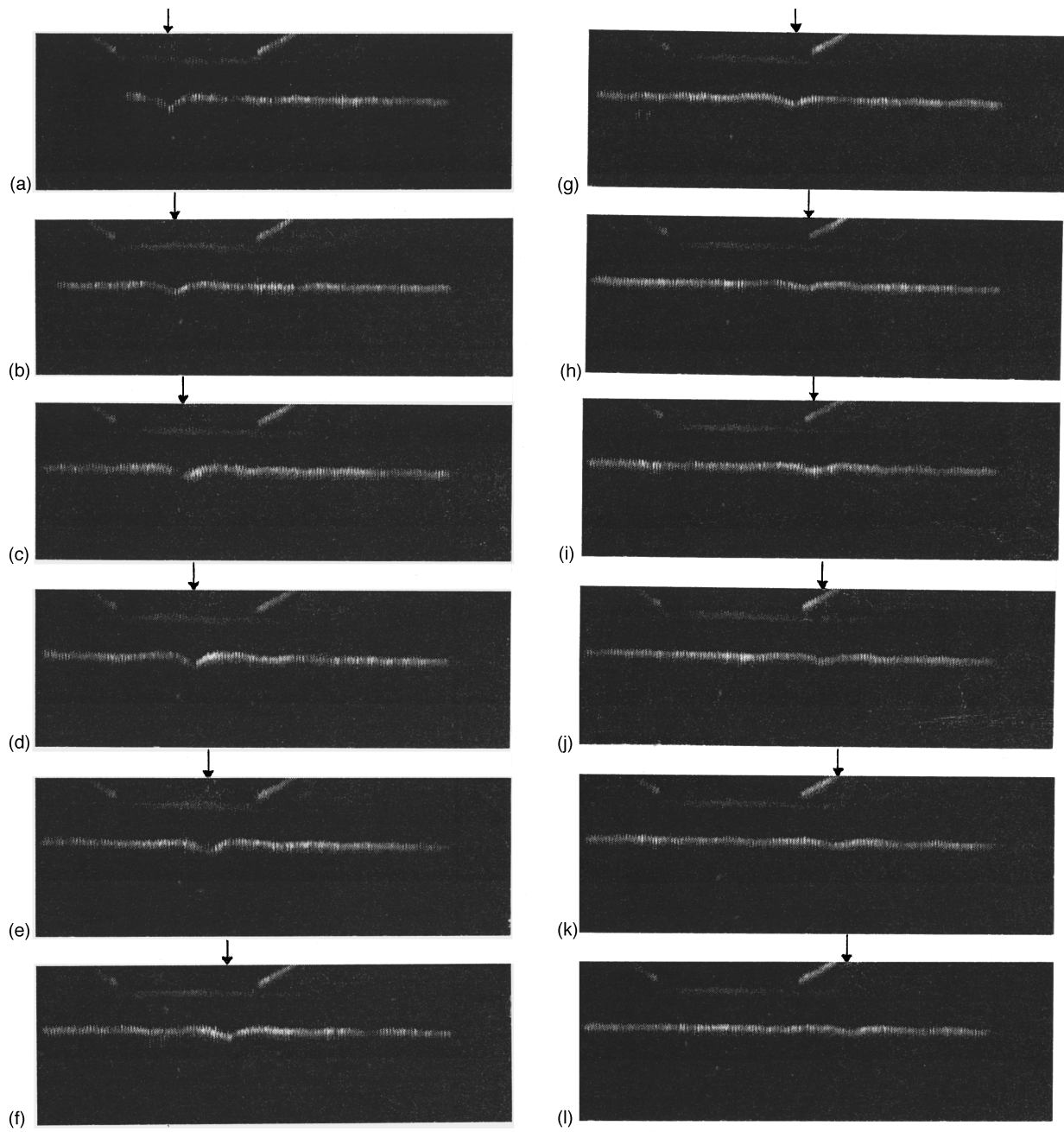


FIG. 9. Successive profiles of the water surface at intervals of 0.1 s, following the cut-off of air pressure.

(see Ref. 7). In this calculation it was assumed that the wave was irrotational, since the rectified vorticity generated at the free surface is quickly advected away from the main wave by the oncoming steady current.

From Fig. 10 one can see the following:

- (1) The general trend of the plotted points follows the theoretical curve rather well over a time interval of more than 1 s. This interval can be compared to the time-scale of a solitary wave which is of order $(T/g^3)^{1/4}$, that is about 0.017 s.
- (2) There is an apparent oscillation of the observations about the mean trend, with a period of order 0.5 s. This may be due to a relaxation of the solitary wave to dissipative forces: as the amplitude diminishes, so the horizontal

extent of the weave has to increase in inverse proportion.⁴ In other words the shape of the wave envelope has to change, the energy being distributed over an increasingly wide distance. A complete theory for the viscous decay of solitary waves is still lacking.

- (3) To the left of Fig. 10, where the theoretical values of α_{\max} exceed 45° , the theoretical rate of decay is very large, with a time-scale of order 0.1 s instead of 4 s. This may partly explain why it is difficult experimentally to generate very steep solitary waves, at least with the present technique. (Other reasons would include wave instabilities, and the fact that the wave profile becomes less well matched to the exciting pressure distribution.)

In Fig. 11 is plotted the observed horizontal displace-

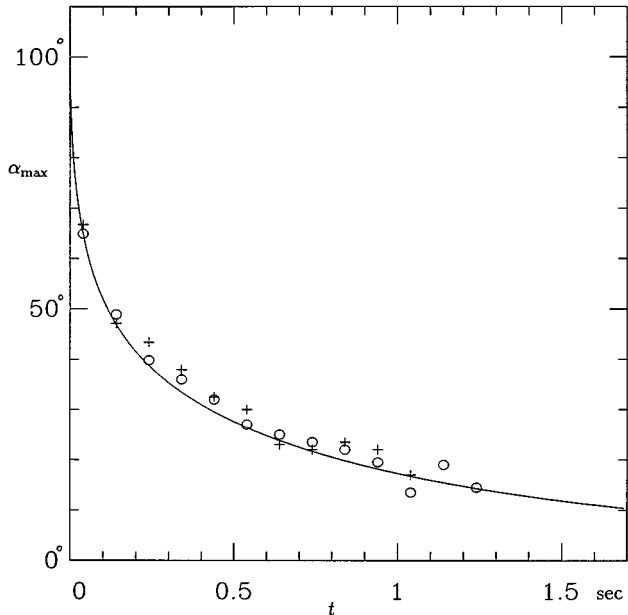


FIG. 10. The maximum slope α_{\max} as a function of the time t . Plotted points: observations. Continuous curve: theory from Eq. (5.1).

ment x of the central wave trough (as indicated by the arrow in each frame). This is compared with a theoretical curve derived from Equation (5.1) by plotting

$$t = - \int_0^E \frac{dE}{D} \quad (5.2)$$

and

$$x = \int_0^t (c - c_0) dt = - \int_0^E (c - c_0) \frac{dE}{D} \quad (5.3)$$

parametrically, with the speed c as parameter. Here c_0 denotes the speed of the waves at time $t=0$, which is assumed to be that of the steady current.

Again it can be seen that the measured displacement follows the theoretical curve fairly well. The limiting slope of the theoretical curve for large values of t corresponds to a speed $(c_l - c_0)$, where c_l is the phase-speed of linear waves, that is $c_l = (4gT)^{1/4} = 23.3$ cm/s.

VI. CONCLUSIONS

A stationary, thin jet of air impinging on the surface of a steady stream can produce a local disturbance in the form of a solitary capillary-gravity wave (soliton) on deep water, provided the current speed is close to the theoretical speed of the wave. With zero current the displacement due to the same jet is negligible. Thus we may speak of the resonant excitation of the solitary wave.

The appropriate current speed is slightly less than $(4gT)^{1/4}$, the minimum speed of small-amplitude waves, and

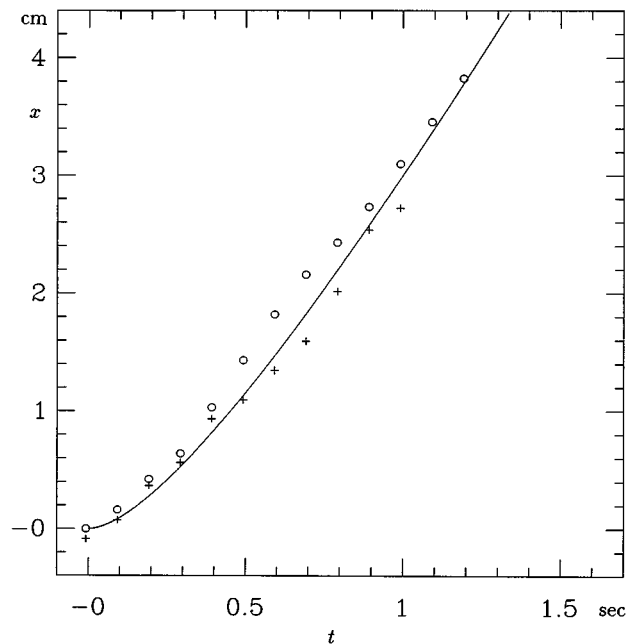


FIG. 11. Horizontal displacement x of the central wave trough as a function of the time t . Plotted points: observations. Continuous curve: theory from Eqs. (5.2) and (5.3).

is a decreasing function of the wave amplitude, in accordance with the theory of free solitary waves.

When the excitation is removed, the solitary wave continues to propagate as a free wave decaying under the action of viscosity. Observations show that the wave accelerates upstream in accordance with theory.

ACKNOWLEDGMENTS

We are much indebted to Dr. Charles S. Cox for assistance in the design and construction of the flume described in Sec. II. The fabrication of the flume was carried out by John Lyons in the Hydraulics Laboratory of the Scripps Institution of Oceanography. This work has been supported by the N.S.F. under Grant No. OCE-93-14308 and by the Office of Naval Research under Grant No. N00014-95-1-0006.

¹M. S. Longuet-Higgins, "Limiting forms for capillary-gravity waves," *J. Fluid Mech.* **194**, 351 (1988).

²M. S. Longuet-Higgins, "Capillary-gravity waves of solitary type on deep water," *J. Fluid Mech.* **200**, 451 (1989).

³J.-M. Vanden-Broeck and F. Dias, "Gravity-capillary solitary waves in water of infinite depth and related free-surface flows," *J. Fluid Mech.* **240**, 549 (1992).

⁴M. S. Longuet-Higgins, "Capillary-gravity waves of solitary type and envelope solitons on deep water," *J. Fluid Mech.* **252**, 703 (1993).

⁵X. Zhang and C. S. Cox, "Measuring the two-dimensional structure of a wavy water surface optically: A surface gradient detector," *Exp. Fluids* **17**, 225 (1993).

⁶X. Zhang, "Capillary-gravity and capillary waves generated in a wind-wave tank: Observations and theories," *J. Fluid Mech.* **289**, 51 (1995).

⁷M. S. Longuet-Higgins, "Viscous dissipation in steep capillary-gravity waves," *J. Fluid Mech.* (in press).